Food Sci. Biotechnol. Vol. 17, No. 2, pp. 330 ~ 335 (2008)

Food Science and Biotechnology

Kinetics of Water Vapor Adsorption by Chitosan-based Nanocomposite Films

Eun Ju Seog, Li Zuo, Jun Ho Lee*, and Jong-Whan Rhim[1]

Department of Food Science and Engineering, Daegu University, Gyeongsan, Gyeongbuk 712-714, Korea

[1]*Department of Food Engineering, Mokpo National University, Muan, Jeonnam 534-729, Korea*

Abstract Water vapor adsorption kinetics of 3 different types of chitosan-based films, i.e., control chitosan, chitosan/montmorillionite (Na-MMT), and chitosan/silver-zeolite (Ag-Ion) nanocomposite films, were investigated at temperature range of 10-40°C. In all the films, water vapor is initially adsorbed rapidly and then it comes slowly to reach equilibrium condition. Reasonably good straight lines were obtained with plotting of $1/(m\text{-}m_0)$ vs. $1/t$. It was found that water vapor adsorption kinetics of chitosan-based films was accurately described by a simple empirical model and the rate constant of the model followed temperature dependence according to Arrhenius equation. Arrhenius kinetic parameters (E_a and k_o) for water vapor adsorption by chitosan-based films showed a kinetic compensation effect between the parameters with the isokinetic temperature of 315.52 K.

Keywords: chitosan, montmorillionite (NA-MMT), silver-zeolite (Ag-Ion), nanocomposite films, water vapor adsorption, kinetics

Introduction

Chitosan is derived from the second most abundant naturally occurring biopolymer, chitin, by de-acetylation in the presence of alkali (1,2). Structurally, it is a copolymer consisting of β-(1-4)-2-acetamino-D-glucose and β-(1-4)-2-amino-D-glucose units with the latter usually exceeding 80% (3,4). Chitosan is generally characterized in terms of the degree of de-acetylation and average molecular weight and functional residues with its antimicrobial properties in conjunction with its cationic nature (5,6).

Chitosan has been considered as one of the most promising biopolymers for the preparation of biodegradable/edible packaging films due to its good film forming properties with its non-toxic, biodegradable, biocompatible, and annually renewable nature (6-9). And it has already been widely used in tissue engineering and drug delivery by virtue of its mechanical strength and rather slow biodegradable (10,11). However, the utilization of chitosan films as a packaging application has been limited due to their low water vapor barrier properties caused by their hydrophillic nature (12-14). As one of the promising methods to improve film properties, such as mechanical and water vapor barrier properties, of chitosan films, various types of chitosan-based nanocomposite films including layered silicate clay (e.g., montmorillonite), silver nanoparticle (e.g., nanosilver), and silver containing zeolite (e.g., Ag-Ion) have been developed (15-20). The chitosan nanocomposite films were prepared by using a solvent-casting method by incorporation with different types of nano particles, such as an unmodified montmorillonite (Na-MMT), an organically modified montmorillonite (Cloisite 30B), Ag-zeolite (Ag-Ion), and so on, which were found its tensile strength increased by 7-16% with promising range of antimicrobial activity (16).

The water vapor barrier properties of hydrophilic biopolymer-based films, like chitosan-based films, are significantly influenced by the presence of moisture (13,14). Therefore, an understanding of the water sorption properties of the biopolymer-based films is essential for their application in food packaging system. In the adsorption process water molecules distribute themselves between the vapor phase and the film surface until a state of equilibrium has been reached. This process may be studied by measuring either the equilibrium condition or the rate of approach to equilibrium. The equilibrium condition can be done through determining the water adsorption isotherm, however, isotherm only explains the final equilibrium condition, and it does not explain sorption of water vapor in the middle of the process. The latter one (the rate of approach to equilibrium) is done by means of adsorption curves, which are plots of weight against time at constant relative humidity and temperature. It is desirable to characterize the rate of water adsorption with a single quantity rather than by entire curve. Kim and Rhim (21) characterized the water vapor adsorption behavior of sweet potato starch-based films, but information on kinetic behavior of water vapor adsorption of chitosan-based nanocomposite films is not available in the literature.

The objectives of this study were to provide reliable experimental data regarding water vapor adsorption behavior of chitosan-based nanocomposite films and to identify and test simple relationships to characterize the water vapor adsorption kinetics at different temperatures and certain relative humility.

Materials and Methods

Materials Chitosan (CS-001; Samsung Chitopia, Seoul, Korea), viscosity being 110 cp in a 1% acetic acid solution at 25°C and degree of de-acetylation of 90%, was obtained locally. Sodium montmorillonite (Na-MMT, Nanomer

---

*Corresponding author: Tel: 82-53-850-6535; Fax: 82-53-850-6539
E-mail: leejun@daegu.ac.kr
Received July 20, 2007; accepted October 17, 2007

PGW, lot PC-243-99, 120 mmol/100 g CEC) and silver-zeolite (Ag-Ion) were obtained from Nanocore Inc. (Arlington Heights, IL, USA) and AgIon™ Technologies, Inc. (Wakefield, MA, USA), respectively. Ag-Ion is a mixture of sodium aluminosilicate (zeolite, >75 wt%), silver (2.1-2.8 wt%), zinc (14 wt%), and ammonium, whose mean particle size distribution is less than 5.0 μm. Analytical grade glycerin was purchased from J. T. Baker (Mallinkrodt Baker, Inc., Phillipsburg, NJ, USA).

Preparation of films Chitosan and chitosan-based nanocomposite films were prepared according to the method of Rhim *et al.* (16). For the preparation of control chitosan film, 4 g of chitosan powder were dissolved in a constantly stirred mixture of 1%(v/v) acetic acid aqueous solution (200 mL) and glycerin (1.0 g) by heating for about 20 min at 90°C using a hot plate. The dissolved film solution was strained through 8-layered cheese cloth to remove undiluted debris, then cast onto a leveled Teflon-coated glass plate (24×30 cm). The castings were dried at ambient conditions (about 23°C) for about 48 hr, then peeled off from the glass plates.

Chitosan-based nanocomposite films were prepared by reinforcing with 2 different types of nanoparticles, such as Na-MMT and Ag-zeolite. First, 5% of each type of nanoparticle (w/w, relative to chitosan on a dry basis) was dispersed in a 1% acetic acid solution (200 mL) by vigorously mixing for 1 hr using a magnetic stirrer and then sonicated for 30 min at 60°C in a bath type ultra sound sonicator (FS14H; Fisher Scientific, Pittsburg, PA, USA) to obtain a nanoparticle solution. Four g of chitosan powder were then dissolved into the nanoparticle solution after adding 1 g of glycerin, and all was heated for about 20 min at 90°C using a hot plate mixer. The solution was sonicated for an additional 10 min at 60°C, after which the solution was strained and cast following the same procedure for the preparation of chitosan film.

All of the films were cut into 2.54×2.54 cm samples and dried in a vacuum oven (Eyela VOS-301SD; Rikakikai Co., Ltd., Tokyo, Japan) at 50°C, 0.1 MPa for 3 days to reduce the initial moisture content. The dried samples were then used for the determination of water vapor adsorption from 10 to 40°C at different water activity.

Moisture content Film samples were weighed (±0.0001 g) into aluminum dishes and dried in an air-circulating oven (Mechanical convection oven, DMC-122SP, 021001-03; Daegil Engineering Co., Seoul, Korea) at 105°C for 24 hr. Moisture content was determined as percentage of initial film weight lost during drying and reported on a dry basis. Duplicate measurements of moisture content were obtained for each type of film with individually prepared films as replicated experimental units.

Water vapor adsorption Tests of water vapor adsorption of the films were conducted at relative humidity of 52-63% from 10 to 40°C. About 0.1 g of each film specimen was placed on an aluminum dish (Disposable Al Dish D57; Korea Ace Scientific Co., Seoul, Korea). A temperature humidity testing chamber (KCL-2000A·2000W; Rikakikai Co., Ltd.) were used to get the indicated temperature within ±0.5°C. Increase in weight of the film specimens during the water vapor adsorption process was recorded during 48 hr and the weight gain in g H_2O/g dry solid was used for the further analysis.

Water activity measurement Sodium bromide (NaBr: D.S.P. GR reagent grade; Duksan Pure Chemical Co., Ltd., Ansan, Korea) was used to obtain desired relative humidity. The salts were dissolved in hot distilled water (100°C) and cooled to each test temperature for crystallization to form a saturated slush (20). Water activity inside the vacuum desiccators after attaining equilibrium with each saturated salt solution was determined using a thermo recorder (TR-72U; T&D Corporation, Matsumoto City, Japan).

Data analysis Temperature dependency of water activity was tested using the Clausius-Clapeyron equation:

$$\frac{d\ln A_w}{d(1/T)} = \frac{-\Delta H}{R} \tag{1}$$

where Aw is the water activity, T is the absolute temperature (K), ΔH is net isosteric heat of sorption (J/mol) and R is the universal gas constant (8.314 J/mol·K).

Water vapor adsorption curves of the chitosan-based films were obtained by plotting increase in weight (g) due to water vapor sorption expressed in g H_2O/g dry solid against adsorption time (hr). The rate constant of water sorption process was determined by a linear form as below:

$$\frac{1}{m-m_0} = \frac{1}{k(m_e-m_0)t} + \frac{1}{m_e-m_0} \tag{2}$$

This relationship has been used to predict the water sorption by chitosan films (21,23), where m_e and m_0 are the saturation moisture content and the initial moisture content, respectively, and k is the rate constant of the sorption process. The inverse of $m-m_0$ ($1/(m-m_0)$) was plotted against inverse of time ($1/t$) following the Eq. 2 to get a straight line. The reaction rate constant was determined by taking inverse of the slope value. The temperature dependency of k value was determined by an Arrhenius-type equation as the following:

$$k = k_0 \exp(-E_a/RT) \tag{3}$$

where k_0 is a pre-exponential factor, E_a is the activation energy for hydration process, R is the universal gas constant (8.314 J/mol·K), and T is the absolute temperature (K). The values of activation energy have the same order of magnitude as encountered in hydration of biological materials (23). In case of chitosan-based nanocomposite films the activation energy for hydration was investigated depending on the several temperatures at certain water activity to compare the effect of the different particle materials on the water vapor adsorption of chitosan-based film.

Results and Discussion

Properties of films All the chitosan and chitosan-based nanocomposite films were flexible and transparent as cellophane. Properties of the films such as apparent surface color, mechanical and water vapor barrier properties as

Table 1. Water activity values of saturated salt (NaBr) solution at different temperatures

Temp. (°C)	Aw	ΔH[1] (kJ/mol)
10	0.63	4.504
20	0.58	
30	0.56	
40	0.52	

[1] Net isosteric heat of sorption.

well as degree of intercalation of nanocomposite films using X-ray diffraction patterns are well documented in the literature (16). Rhim *et al.* (16) showed through X-ray diffraction analysis that a certain degree of intercalation was formed in the Na^+-MMT/chitosan nanocomposite films. In consequence, mechanical and barrier properties of the chitosan films were improved through the formation of nanocomposite films, that is, the tensile strength increased from 32.9±0.7 MPa for the neat chitosan films to 35.1±0.9 and 38.0±3.4 MPa for Na-MMT/chitosan and Ag-Ion/chitosan nanocomposite films, respectively, and the water vapor permeability of the chitosan film decreased from $(1.31\pm0.07)\times10^{-9}$ to $(0.98\pm0.15)\times10^{-9}$ and $(0.96\pm0.05)\times10^{-9}$ $g\cdot m/m^2\cdot sec\cdot Pa$, respectively.

Water activity of saturated salt solution Water activity values of saturated salt (NaBr) solution were shown in Table 1. The saturated NaBr solution was chosen to test the water vapor absorption by the film at the middle range of Aw, which ranged 0.52 to 0.63 at the temperature range tested. The water activity values of saturated salt solutions decreased with an increase in temperature. The temperature dependency of water activity followed the Clausius-Clapeyron equation (Eq. 1). Regression analysis using the least square method on ln Aw versus 1/*T* for the salt solution gave following relationship:

$$\ln A_w = 541.752\cdot(1/T) - 2.380 \quad (R^2 = 0.981) \qquad (4)$$

The net isosteric heat of sorption for NaBr saturated salt solutions determined from the slope of the regression line was 4.504 kJ/mol. Labuza *et al.* (24) showed that the effect of temperature on the Aw of salt solution was dependent on the saturated salt solutions used, of which the net isosteric heat of sorption were in the range of 1.21-7.16 kJ/mol depending on the salt solution.

Water vapor adsorption curves Water vapor adsorption behaviors of control chitosan and chitosan/clay nanocomposite films at different temperatures were shown in Fig. 1. The rapid initial moisture sorption followed by slower adsorption at later stages, due to the filling capillaries of the surface of the films (21,25), were observed from the curves. All the chitosan-based films showed the similar adsorption behavior as sweet potato starch-based edible film (21) and soy protein film (26). During the process of moisture sorption preceded, the adsorption rate decreased probably due to the filling of free capillary with water vapor.

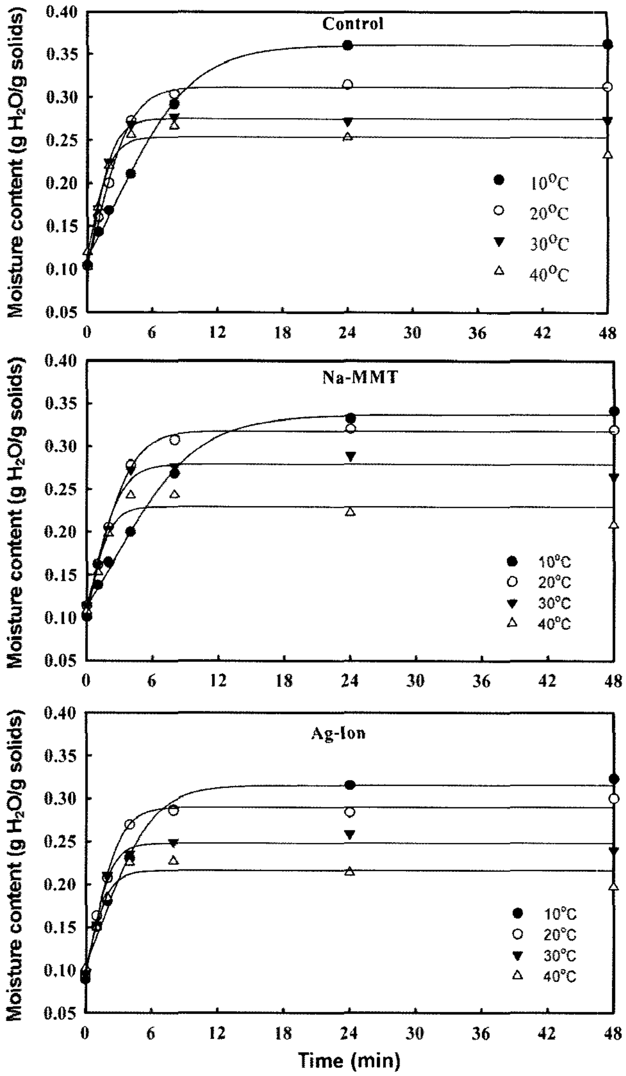

Fig. 1. Water vapor adsorption behaviors of control and chitosan-based films at different temperatures.

The saturation moisture content (m_e) was influenced by the source of films. The results were shown in Table 1. In the previous study the nano particles were dispersed homogeneously throughout the chitosan polymer matrix and the intercalation in the Na-MMT incorporated films was higher than that in Ag-Ion (16). The certain degree of intercalation which formed in the nanocomposite films had a certain effect on the water vapor adsorption capacity. Chitosan/Ag-Ion nanocomposite film showed the least water vapor adsorption capacity among the films tested at different temperature. The moisture sorption curves also indicated that the vapor adsorption decreased with the temperature increased as observed in different type of biopolymer films (21).

Water vapor adsorption rate The inverse of $m-m_0$ $(1/(m-m_0))$ was plotted against inverse of time (1/*t*) following the Eq. 2 to get a straight line. The reaction rate constant was determined by taking inverse of the slope value. From water vapor adsorption curves, it was found that water vapor adsorption rate varied depending on the kind of samples and temperature. By plotting $1/(m-m_0)$ against $1/t$ based on Eq. 2, water vapor adsorption rate constant was determined. Figure 2 shows typical kinetic plot lines for water vapor adsorption of different chitosan-based films.

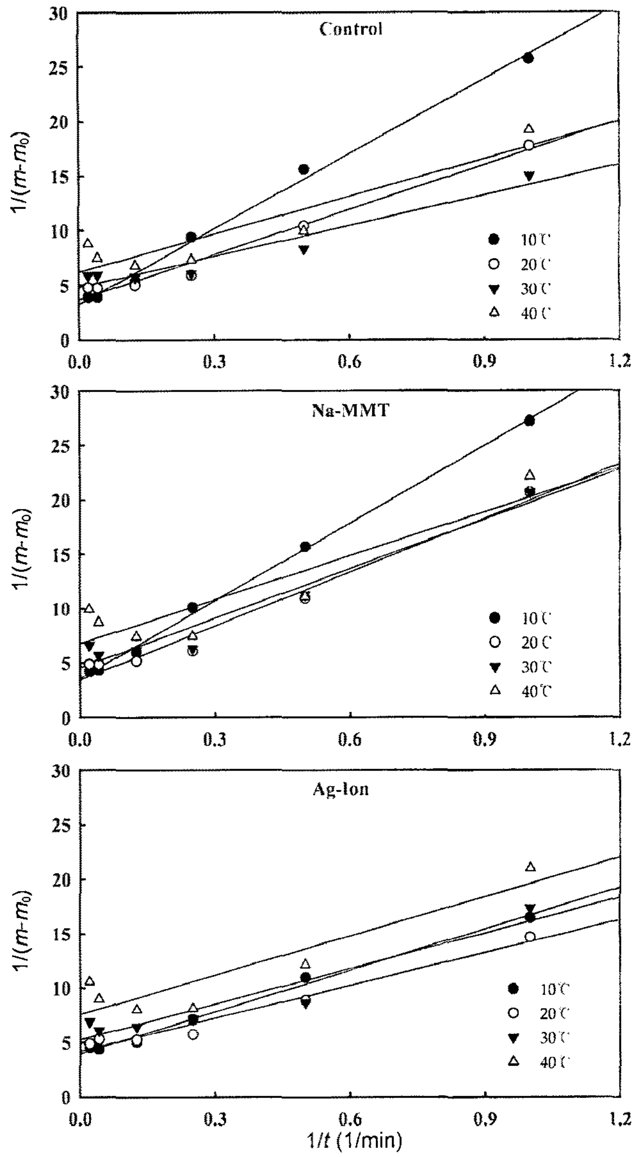

Fig. 2. Adsorption kinetics of chitosan-based films determined at different temperatures.

Reasonably good straight lines were obtained with such simple plot of $1/(m-m_0)$ vs. $1/t$ with high R^2-values. From the slope value of the lines, water vapor adsorption rate constants were calculated. The rate constants for the films were summarized in Table 2. The water vapor absorption rate for all the films increased with temperature, which is in good agreement with the finding of other researchers (21). Chitosan/Ag-Ion nanocomposite film showed the highest water vapor adsorption rate among the films tested except at 30°C.

Effect of temperature By using the Arrhenius-type equation in Eq. 3, temperature dependency of the water vapor adsorption rate of chitosan-based films was determined. The temperature dependency of water vapor adsorption rate is shown in Fig. 3. The good linear relationship with high R^2 values of 0.927, 0.978, and 0.986 was obtained for control chitosan, chitosan/Na-MMT, and chitosan/Ag-Ion nanocomposite films, respectively, was obtained. This result indicated that Arrhenius model can be appropriately used to describe the temperature dependency of the sorption rate of the films. The Arrhenius kinetic parameters, activation energy (E_a), and the pre-exponential factor (k_o) for the water vapor adsorption by the films were determined by linear regression method and results were summarized in Table 3. In general, the temperature dependency of water vapor adsorption by a polymeric film is known to be dependent on various factors like hydrophilicity and free volume of the polymer matrix (27). In the present study, activation energy varied depending on the source of films. As a whole, activation energies of control film were higher than the others, so it is expected to be more sensitive to temperature variation than other chitosan based nanocomposite films.

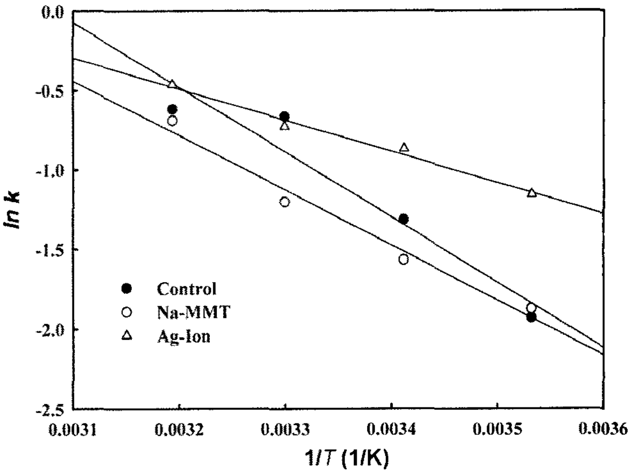

Fig. 3. Temperature dependency of water vapor adsorption of chitosan-based films.

Kinetic compensation effect As noted above, the Arrhenius kinetic parameters (E_a and k_o) for water vapor adsorption rate varied depending on the source of films and water activity. Numerical values of kinetic parameters are changed due to the reaction conditions such as reactant concentration, pH, water activity, and so on; however, the Arrhenius kinetic parameters (E_a and k_0) for water vapor adsorption rate usually show linear relationship between ln k_0 and E_a, which is known as kinetic compensation effect (28,29). The relationship between E_a and k_0 for water vapor adsorption rate of the chitosan-based films was shown in Fig. 4. The following linear relationship was obtained from linear regression analysis:

$$\ln k_0 = 0.381\ E_a - 0.488 \quad (R^2 = 0.998) \qquad (5)$$

This result shows a highly linear relationship between the kinetic parameters (i.e., ln k_0 vs. E_a), which indicates a systematic variation of one parameter depending on the other. Such a systematic variation between the kinetic parameters is known as a kinetic compensation effect (30), which is usually observed in a family of reactions with same reaction mechanism. The compensation relation suggests that the activation energy (E_a) and the pre-exponential factor (k_0) are not independent of one another and any change in the activation energy is compensated by changes in the pre-exponential factor. This unique

Table 2. Reaction rate constants for water vapor adsorption of chitosan-based films at different temperatures

Chitosan films	Temp. (°C)	Reaction rate constant, *k* (g H_2O/g dry solid/min)	Saturation moisture content, m_e (g H_2O/g dry solid)	R^2
Control	10	0.145	0.362	0.995
	20	0.269	0.313	0.981
	30	0.515	0.274	0.931
	40	0.539	0.234	0.855
Na-MMT	10	0.154	0.342	0.998
	20	0.209	0.320	0.974
	30	0.300	0.265	0.946
	40	0.501	0.209	0.819
Ag-Ion	10	0.314	0.323	0.993
	20	0.419	0.300	0.973
	30	0.483	0.240	0.908
	40	0.629	0.197	0.839

Table 3. Kinetic parameters for water vapor adsorption of chitosan-based films

Chitosan films	k_0 (g H_2O/g dry solid/min)	E_a (kJ/mol)	R^2
Control	3.034×10^5	34.045	0.927
Na-MMT	2.884×10^4	28.721	0.978
Ag-Ion	3.409×10^2	16.427	0.986

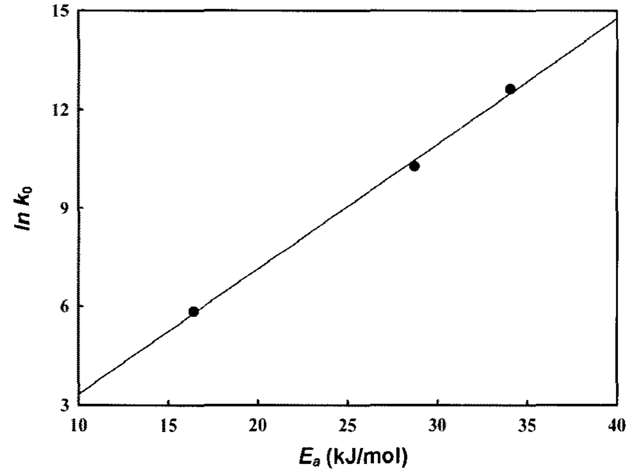

Fig. 4. Kinetic compensation effect of water vapor adsorption of chitosan-based films.

relationship between k_0 and E_a for a family of related reactions, can be utilized for prediction of reaction rates or other kinetic parameters (31). The linear relationship between these kinetic parameters implies the existence of a unique temperature called the iso-kinetic temperature (T_c) (30). At this temperature, the rate constants of all reactions in the series have the same value. The iso-kinetic temperature is usually calculated based on the slope in the ln k_0 vs. E_a plot using the relationship of slope = $1/(RT_c)$.

According to Arrhenius curves, the thermal activation compensation or isokinetic temperature was obtained by graphical extrapolation. The isokinetic temperature represents a temperature at which all reactions of the series should proceed at the same rate, mathematically a reflection of the dependence of activation energy on the temperature (32, 33). From the slope, the isokinetic temperature of water vapor adsorption for chitosan-based films determined from the slope value was found to be 315.52 K, which is in good agreement with the published results (21) with a high degree of linear correlation.

References

1. Shahidi F, Arachchi JKV, Jeon YJ. Food application of chitin and chitosan. Trends Food Sci. Tech. 10: 37-51 (1999)
2. No HK, Meyers SP, Prinyawiwatkul W, Xu Z. Applications of chitosan for improvement of quality and shelf life of foods: A review. J. Food Sci. 72: R87-R100 (2007)
3. Harish Prashanth KV, Tharanathan RN. Chitin/chitosan: Modifications and their unlimited application potential - an overview. Trends Food Sci. Tech. 18: 117-131 (2007)
4. Muzzarelli RAA. Chitosan-based dietary foods. Carbohyd. Polym. 29: 309-316 (1996)
5. Knorr D. Use of chitinous polymers in food. Food Technol.-Chicago 38: 85-97 (1984)
6. Srinivasa PC, Ramesh MN, Kumar KR, Tharanathan RN. Properties of chitosan films prepared under different drying conditions. J. Food Eng. 63: 79-85 (2004)
7. Zhang M, Li XH, Gong YD, Zhao NM, Zhang XF. Properties and biocompatibility of chitosan films modified by blending with PEG. Biomaterials 23: 2641-2648 (2002)
8. Park SY, Marsh KS, Rhim JW. Characteristics of different molecular weight chitosan films affected by the type of organic solvents. J. Food Sci. 67: 194-197 (2002)
9. Chung D, Kim SM, KIm WT, Shin IS, Park H. Characteristics of films based on chitosan isolated from Todarodes pacificus. Food Sci. Biotechnol. 14: 433-436 (2006)
10. Ma J, Wang H, He B. A preliminary *in vitro* study on the fabrication and tissue engineering applications of a novel chitosan bilayer material as a scaffold of human neofetal dermal fibroblasts. Biomaterials 22: 331-336 (2001)
11. Dhanikula AB, Panchagnula R. Development and characterization of biodegradable chitosan films for local delivery of paclitaxel. AAPS J. 6: 1-27 (2004)
12. Rhim JW, Weller CL, Ham KS. Characteristics of chitosan films as affected by the type of solvent acid. Food Sci. Biotechnol. 7: 263-268 (1998)
13. Gennadios A, Park HJ, Weller CL. Relative humidity and temperature effects on tensile strength of edible protein and cellulose ether films. T. ASAE 37: 1867-1872 (1993)
14. Gontard N, Guilbert S, Cuq J. Water and glycerol as plasticizer affect mechanical and water vapor barrier properties of an edible

wheat gluten film. J. Food Sci. 58: 206-211 (1993)

15. Wang X, Du Y, Yang J, Wang X, Shi X, Hu Y. Preparation, characterization, and antimicrobial activity of chitosan/layered silicate nanocomposites. Polymer 47: 6738-6744 (2006)
16. Rhim JW, Hong SI, Park HM, Ng PKW. Preparation and characterization of chitosan-based nanocomposite films with antimicrobial activity. J. Agr. Food Chem. 54: 5814-5822 (2006)
17. Rhim JW. Effect of clay concentration on mechanical and water barrier properties of chitosan-based nanocomposite films. Food Sci. Biotechnol. 15: 925-930 (2006)
18. Lin KF, Hsu CY, Huang TS, Chiu WY, Lee YH, Young TH. A novel method to prepare chitosan/monymorillonite nanocomposites. J. Appl. Polym. Sci. 98: 2042-2047 (2005)
19. Xu Y, Ren X, Hanna MA. Chitosan/clay nanocomposite film preparation and characterization. J. Appl. Polym. Sci. 99: 1684-1691 (2006)
20. Wang SF, Shen L, Tong YJ, Chen L, Phang IY, Lim PQ, Liu TX. Biopolymer chitosan/montmorillonite nanocomposites: Preparation and characterization. Polym. Degrad. Stabil. 90: 123-131 (2005)
21. Kim JN, Rhim JW. Kinetics of water vapor adsorption by sweet potato starch-based edible films. Food Sci. Biotechnol. 13: 616-621 (2004)
22. Rockland LB. Saturated salt solutions for static control of relative humidity between 5 and 4°C. Anal. Chem. 32: 1375-1376 (1960)
23. Singh BPN, Kulshrestha SP. Kinetics of water sorption by soybean and pigeonpea grains. J. Food Sci. 52: 1538-1541, 1544 (1987)
24. Labuza TP, Kaanane A, Chen JY. Effect of temperature on the moisture sorption isotherms and water activity shift of two dehydrated foods. J. Food Sci. 50: 385-391 (1985)
25. Rhim JW. Hydration kinetics of soybeans. Food Sci. Biotechnol. 12: 303-306 (2003)
26. Cho SY, Rhee C. Sorption characteristics of soy protein films and their relation to mechanical properties. Lebensm.-Wiss. Technol. 35: 151-157 (2002)
27. Avramova N. Effect of structure on sorption and diffusion processes in polyamide 6, Part 1: Activation energy and thermodynamic parameters of water desorption in oriented and unoriented polyamide 6. J. Appl. Polym. Sci. 106: 122-129 (2007)
28. Özilgen M. Enthalpy-entropy and frequency factor-activation energy compensation relations for diffusion in starch and potato tissue. Starch-Starke 45: 48-51 (1993)
29. Rhim JW. Kinetic compensation relations for texture changes in sweet potatoes during heating. Food Sci. Biotechnol. 11: 29-33 (2002)
30. Rhim JW, Nunes RV, Jones VA, Swartzel KR. Appearance of a kinetic compensation effect in the acid-catalyzed hydrolysis of disaccharides. J. Food Sci. 54: 222-223 (1989)
31. Aguerre RJ, Suarez C, Violaz PE. Enthalpy-entropy compensation in sorption phenomena: Application to the prediction of the effect of temperature on food isotherms. J. Food Sci. 51: 1547-1549 (1986)
32. Exner O. Determination of isokinetic temperature. Nature 227: 366-367 (1970)
33. Peled A, Schein LB. The thermal activation compensation effect and the isokinetic temperature relation to physical models. Phys. Scripta 44: 304-309 (1991)